8th Australasian Congress on Applied Mechanics, ACAM 8
23-26 November 2014, Melbourne, Australia

Experimental investigation of thin metal sheets under tension-compression cyclic loading

Z.L. Kowalewski[1*], L. Dietrich[1], G. Socha[2],

[1]*Institute of Fundamental Technological Research, ul. Pawińskiego 5B, 02-106 Warsaw, Poland*

[2]*Institute of Aviation, Al. Krakowska 110/114, 02-256 Warsaw, Poland*

[*]*Corresponding author. Email: zkowalew@ippt.pan.pl*

Abstract: Strength and durability of thin-walled structures are usually calculated with the use of computer simulations. To perform such simulations using Finite Element Method the characteristics of a material subjected to monotonic tension/or compression and tension-compression cyclic loading are necessary for example. Experimental determination of such kind of characteristics is usually performed on specimens cut out from metal or composite thin sheet. Problems associated with material testing on flat specimens under large deformation are discussed in detail by this paper. In the first part, a short review of the anti-buckling fixtures developed up to now is given. Several representative solutions including the applied design are discussed, with special emphasis on the technique limitations. In the second part, the results of investigations carried out on steel and brass using the new fixture for the flat specimens testing are presented.

Keywords: fixture, large deformations, tension-compression tests, thin metal sheet

1 Introduction

Problems associated with material testing on flat specimens under compression within large deformation range procure many difficulties. It seems that the buckling is regarded as the most significant. Among many important phenomena observed during tests carried out on the flat specimens, which should be taken into account, one can distinguish:

- changes of the hardening modulus of a material due to variation of the loading direction,
- strain-hardening stagnation observed after change of the loading direction,
- relationship between strain amplitude and stress saturation,
- changes of the elastic modules due to cyclic loading.

Templin [1] developed one of the first fixtures dedicated for uniaxial compression of flat specimens. In this fixture, a specimen was inserted between the steel rolls side-supporting it by spring loading. A disadvantage of the method was the contact point between rolls and specimen leading to a local deformation of the material tested, thus disturbing its characteristic to be determined.

The most popular designs of the side-supporting fixture [2-6] were built in the form of rigid blocks applying normal pressure to the flat specimen. Such rigid blocks were usually loaded perpendicularly to the specimen's surface using a spring or screw. Various modifications of such fixture differ in design of supporting blocks, side loading mechanism, strain measurement and test load application method. For all the fixture versions a specimen was longer than the side-supporting blocks by an amount necessary to obtain the required strain. Simultaneously, this amount was limited by the possibility of buckling. Fulfilling of two compromising requirements led to limit a strain range. On the other hand, the strain range was also dependent on the specimen thickness which, in the case of very thin sheet, could limit significantly an attainable compressive deformation. As the matter of fact, a usage of this kind of fixtures reduced an active (gage) length of the specimen.

Dietrich and Turski [7] elaborated in 1978 another solution of the side-supporting fixture. The main advantage of this design was an ability to support the entire specimen gage length during a test. This is due to the fact that side-supporting block was able to change its length together with a gradual shortening of the specimen during compression. Detailed description of the fixture was given in the monograph published in 1990 [8]. The fixture is shown in Fig. 1. The main principle of operation is explained in Fig. 2, where two expanded views of parts of the fixture are shown. Maximum and minimum height of the compression fixture is given in Fig. 1. A torque wrench was used for clamping screws during mounting of specimen in the fixture. A side-support of the specimen was realized by two

sets of thin plates perpendicular to specimen's surface supporting its both sides. Each set, consisting the same type of plate, was positioned by two pins: the first was inserted into pin-hole at one end of the plate and the second was inserted into U-shape cut on the opposite side of the plate. Neighboring plates were rotated with respect to each other by an angle equal to 180 deg, Fig. 2. Upper and lower yoke supported both pins. The screws connecting two parts of the yoke allowed an adjustment of the fixture to fit specimen's thickness.

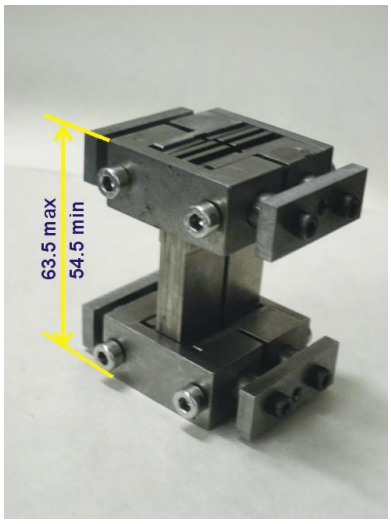

Figure 1: A special fixture for compressive tests which changes its height as the specimen elongates or shortens

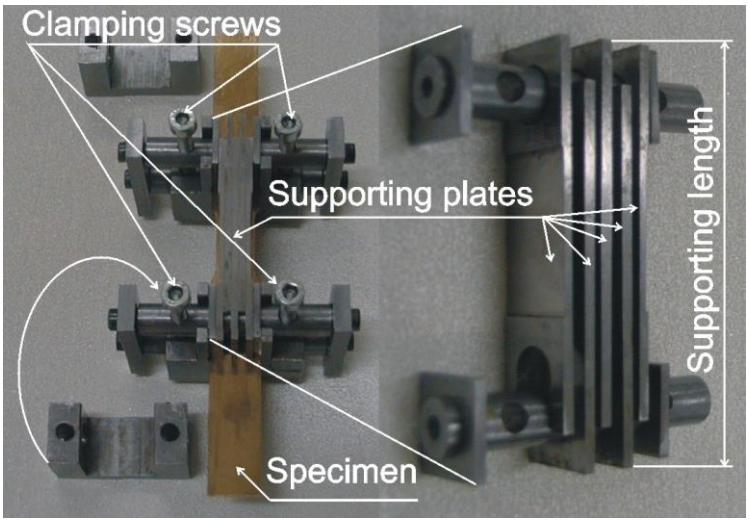

Figure 2: Expanded views of supporting plates and the fixture with mounted specimen and four clamping bolts which establish force of friction between supporting plates and surface of specimen during tests

Kuwabara et al. [9, 10] proposed in 2009 a similar design of the fixture with two comb-like sliding blocks supporting specimen. A part of the block with comb-like cuts supported only the gage section of specimen, while the rigid block supported the remaining part of specimen. It was positioned horizontally between the upper and lower supporting blocks, wherein at the same time a weight of the upper block or additional hydraulic actuator protected the specimen against buckling.

Cao et al. [11] proposed in 2009 a solution of the side-supporting fixture implementing sliding blocks with angular chamfers. Two such blocks joined by the spring and setup to form a rectangle of varying length were located on each side of the flat specimen. Two similar blocks, located on opposite sides of the specimen, were joined with the use of screws enabling application of side-load preventing specimen against the buckling. The spring joining sliding blocks with angular chamfers was initially stretched to overcome a friction between the supporting blocks and specimen on the one hand, and to enable a height increase of two sliding blocks during tensile loading and to fit specimen on the other.
In this paper, a modified version of the fixture developed in 70's [7] was applied to execute experimental investigations of thin metal sheets under tension-compression cyclic loading. It enables application of cyclic tension-compression to the flat specimen in a wide strain range due to coupling of the side-supporting blocks with the standard grips of the testing machine. Design from 70's could have been used only for monotonic compression since supporting blocks once shortened remained in this position. Another important advantage of the proposed design is the ability of monitoring a friction force between the specimen and supporting blocks, which allows avoiding an error during stress determination.

2 Experimental details

2.1 Details of experimental procedure

All tension-compression tests were carried out on thin sheet specimens with nominal thickness equal to 1 mm using the fixture that will be briefly presented in the section 2.2. Dimensions of the specimen are shown in the Fig. 3.

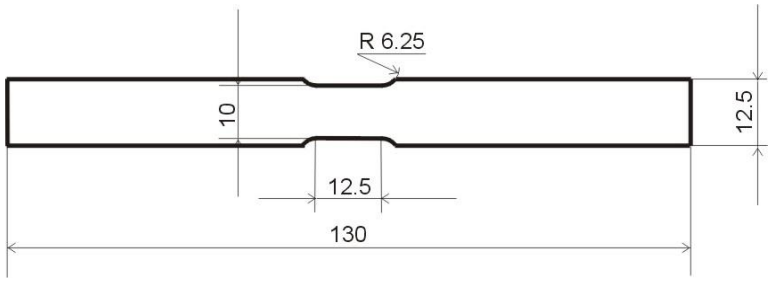

Figure 3: Specimen manufactured from 1 mm thickness sheets of the steel and brass

Materials tested were the 08J steel and M63 brass used in deep-drawing processes. The chemical compositions of materials are presented in Tables 1 and 2 according to Polish Standards.

Table 1: Chemical composition of the 08J steel

C	Si	Mn	P	S	Cr	Ni	Cu	N_2	O_2	Al
max 0.08	max 0.03	0.20÷ 0.45	max 0.025	max 0.030	max 0.10	max 0.10	max 0.10	0.01	0.030	0.02÷ 0.07

Table 2: Chemical composition of the M63 brass (CW508L notation according to EN)

Cu	Ni	Fe	Pb	Zn
62÷64%	max 0.30%	max 0.10%	max 0.10%	rest

2.2 Fixture for tension-compression tests within large deformation range

The main principle of the fixture assembly is explained in Fig. 4 where engineering drawing of the fixture is presented. It shows the fixture with mounted specimen and four clamping screws which establish friction force between the supporting plates and surface of specimen during tests. A torque wrench was used for clamping screws during mounting of specimen in the fixture. Values of the torque moment were established by trial and error method in the preliminary tests. Three sub-assemblies of the device can be distinguished, Fig 4. The first consists of the side-supporting plates set (2, 3, 4, 8 and 9), connecting pins and two pairs of yokes (5, 6 and 7) making two sliding blocks on both sides of the specimen (1). The side-supporting blocks attached to the specimen gauge part are composed in the form of thin plates with circular hole at one side and rectangular cut with semicircular end on the other. Neighboring plates are rotated with respect to each other by an angle equal to 180°, similar to the fixture design shown in Fig. 2. A pin fixed in the yoke joins thin plates with the same position. This assembly forms a variable-length side-supporting block attached to the gauge part of specimen changing length under applied loading. The length of a rectangular cut at one set of supporting plates and the overall length of those plates limit the strain range that can be executed. This is exactly the same design of the side-supporting block, as that developed in 1978 [7]. The side-supporting block consists of several internal full-length plates. The device is equipped also with the external short plates of the same thickness, and therefore, an adjustment of the side-supporting block can be easily performed to fit the specimen width, appropriate to a load capacity of the testing machine. A length of the specimen inserted between the supporting blocks is longer than that of the blocks by an amount equal to twice the height of the gripping part (approximately equal to wedge length). The gripped part of the specimen is held by the wedges (13) comprising standard grip assembly and operated thanks to a hydraulic pressure. The complete assembly of the sliding block is fixed to the testing machine using the standard gripping system. The connecting plates (11) couple the upper and lower yokes with the fixture foundations. A special lock is machined in the connecting plate to fit yoke assembly. It allows a transmission of the axial force from the fixture foundation to yoke. The screws (15) in the yoke are slightly tightened, thus allowing a movement of the first yoke (6) with respect to a second yoke (7) enforced by the specimen thickness variation during a test. The screws (14) in the fixture foundations (12) are tightened strongly, so that a frictional transmission of the loading from the foundations (12) to the connecting plates (11) can be attained. More details of this device can be found in [12].

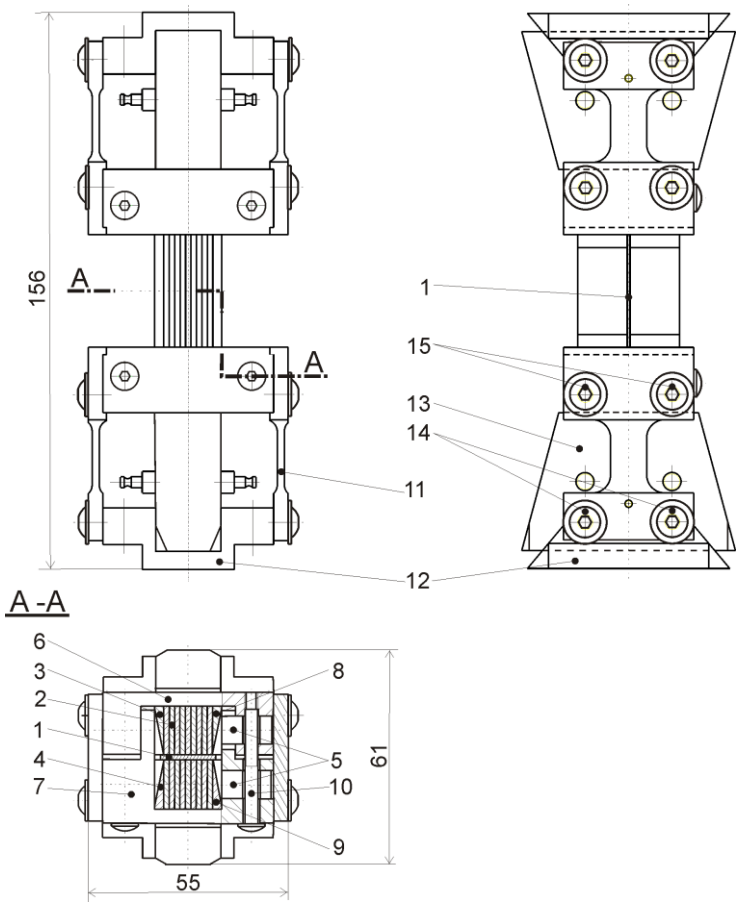

Figure 4: Engineering drawing of the fixture with overall dimensions and numbered component parts as seen in front, side and from top side

2.3 Experimental programme

All loading ramps during tests were carried out under displacement control with additional conditions on the engineering strain or total loading. The testing programme for cyclic tension - compression up to the required value of strain first in tension and next in compression consists of 10 steps. A scheme of the single step is presented in Fig. 5. In the case of tension – compression cycles within a strain range equal to ±0.038 for the steel and ±0.020 for the brass loading started from Ramp 1 under displacement control and went to the final value of 3 mm with a rate of 0.05 mm/s until the required value of strain Limit 1 equal to 0.038 (steel) or 0.020 (brass) was reached. Subsequently, Ramp 2 started and went to value of -3 mm with the same rate equal to 0.05 mm/s until the next Limit 2 in strain equal to -0.038 (steel) or -0.020 (brass) was achieved. A cycle was finished by execution of Ramp 3, which went under displacement control up to the end point equal to 3 mm with a rate of 0.05 mm/s until the last Limit 3 equal to zero strain was reached. The entire procedure was repeated 10 times and in the last cycle number 10 the Limit 3 was defined by force to be equal zero.

Similar programme was assumed in the second type of test realized in a range of strain from zero to -0.058 (steel) or -0.022 (brass). Loading started with Ramp 1 under displacement control and went to the end value of -3 mm with a rate of 0.05 mm/s until the required value of strain Limit 1 equal to -0.058 (steel) or -0.022 (brass) was reached. Next, Ramp 2 started and went to value of +1 mm with the same rate equal to 0.05 mm/s until the next Limit 2 in strain equal to zero (steel) or -0.002 (brass) was achieved. A cycle was completed after execution of Ramp 3, which went under displacement control up to the end point equal to -3 mm with a rate of 0.05 mm/s until the last Limit 3 equal to zero force was reached. The entire procedure was repeated 10 times.

All tests were carried out using extensometer with a range of ±0.2. The load cell was calibrated in the range of ±25 kN. The special set-up for friction force measurements was applied. It consisted of two coupling bars with strain gauges calibrated in the range of ±2 kN.

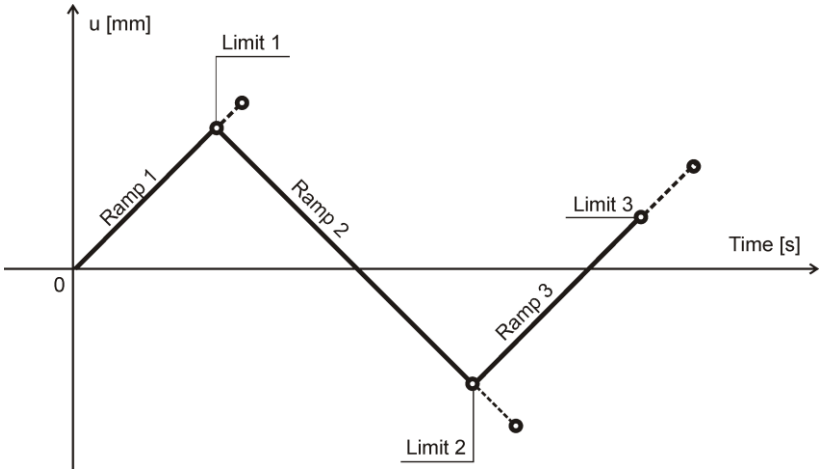

Figure 5: A diagram of a single step of the cyclic tension-compression loading programme

2.4 Preliminary tensile tests

Before tension-compression cycles the standard tensile tests were carried in order to determine mechanical properties of the steel and brass tested. They were performed without application of the anti-buckling fixture. Instead of it, typical grips and mechanical extensometer were used. The tensile characteristics of the steel and brass are presented in Fig. 6.

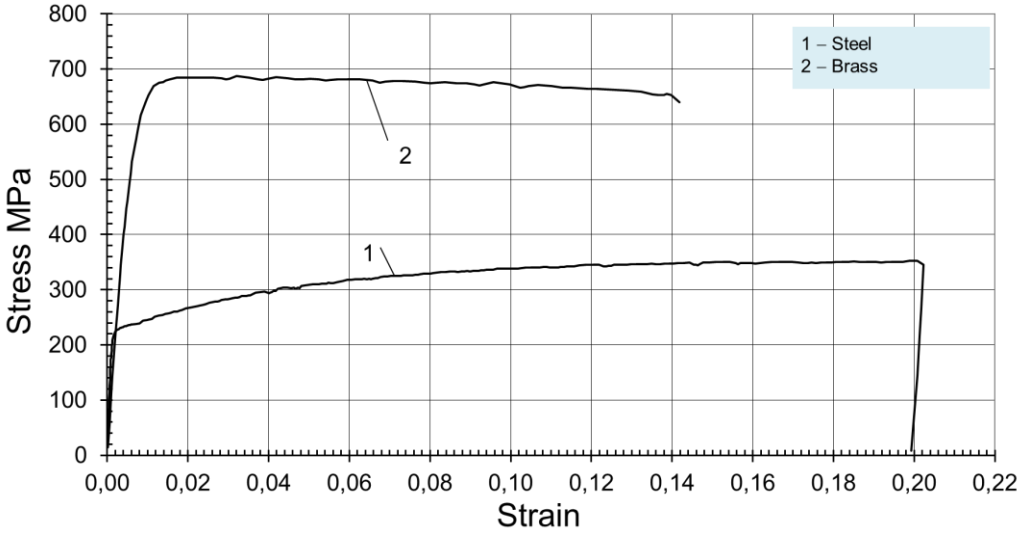

Figure 6: Tensile curves of the steel and brass

On the basis of these curves selected mechanical parameters were determined (Tables 3 and 4).

Table 3: Mechanical parameters of the 08J steel

Young's modulus	Yield point	Tensile strength	Total elongation
GPa	MPa	MPa	%
205	230	350	20

Table 4: Mechanical parameters of the M63 brass

Young's modulus	Yield point	Tensile strength	Total elongation
GPa	MPa	MPa	%
110	550	680	14

The results of tensile tests were also used to validate the experimental data from tension-compression cycles.

3 The results of cyclic tests on steel and brass

The main part of the experimental programme consisted two schemes of cyclic loading. In the first scheme tension-compression cycles were performed for strain level varying between 0.038 and -0.038 in the case of steel or 0.02 and -0.02 for the brass. Ten fully reversible cycles were carried out. The test started in tension direction. Stretching was continued up to the strain level equal to 0.038 (steel) or 0.02 (brass), and then unloading process took place and further loading under compressive conditions up to –0.038 or -0.02 for steel or brass, respectively. Afterwards, unloading process was executed and again stretching up to 0.038 (steel) or 0.02 (brass). The sequence was repeated 10 times. The results for steel are illustrated in Fig. 7 in the form of stress-strain loops.

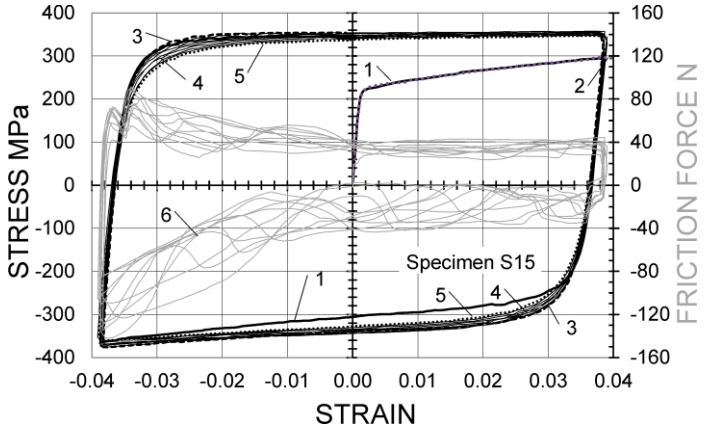

Figure 7: Hysteresis loops of the steel and friction force variation during test

In Fig.7 showing hysteresis loops of the steel, the first cycle is illustrated by solid black line denoted as 1. The tensile stress–strain curve obtained under simple tension without the anti-buckling fixture usage (denoted as 1 in Fig. 6) is also shown in Fig. 7 (gray dotted line denoted as 2). A second cycle is represented by black dashed line (3). The last two cycles - are denoted by black dotted lines (4 and 5). Figure 7 also presents an evolution of the friction force. Variation of the friction force measured by the special force sensor is represented as a function of strain for all cycles (gray lines, denoted as 6). For better clarity, the friction force is also shown as a function of time in Fig. 8 as well as total load for all recorded cycles. The test was in displacement control. Changes of strain, corresponding to the force variations, measured by the extensometer attached in the middle part of the specimen are shown in Fig. 9 for all cycles carried out. The strain amplitude for all cycles was kept constant.

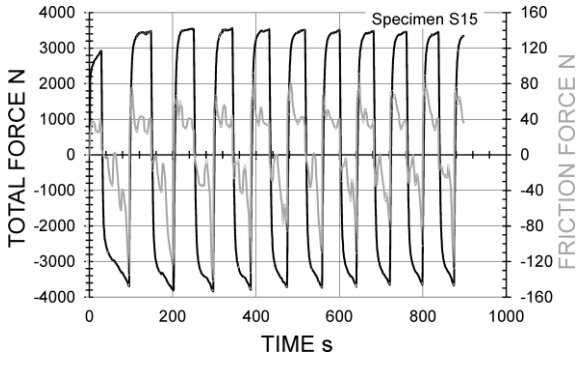

Figure 8: Variation of specimen load and friction force versus time during cyclic loading (steel)

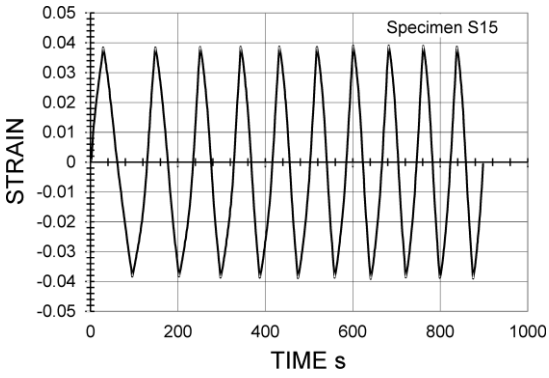

Figure 9: Variation of strain versus time during cyclic loading (steel)

As it is clearly seen, the material exhibited hardening effect reflected by a significant increase of the stress amplitude in the first two cycles, Fig. 8. The experimentally obtained cyclic stress–strain curves of the 08J steel exhibit apparent work hardening stagnation in a certain period of reverse deformation starting from the reverse re-yielding, Fig. 7. This phenomenon is also related to the cyclic

strain-range, as well as mean-strain, dependencies of cyclic hardening characteristics. As pointed out by Yoshida at al. [13], the work hardening stagnation can be caused by the dissolution of dislocation cell walls during a reverse deformation. It can be expressed by the non-isotropic hardening of the bounding surface concept, since in their theoretical model the isotropic hardening of the bounding surface represents the global work hardening due to the formation of stable dislocation structures, such as cell walls. A level of the friction force was monitored during the test. Its variation is presented in Figs.7 and 8. Data concerning the friction force variation were subsequently used to correct the stress-strain diagram by subtracting friction force value from total force to calculate pure specimen load. The friction force has a similar course in all cycles and does not change clearly under tension and grow up at compression due to transversal expansion of specimen, and diminishes in the reverse loading due to transversal shrink of the specimen. It has to be emphasized that the values of friction force were relatively small and they did not change the stress-strain characteristic if only a torque of four clamping bolts, which establish force of friction between the supporting plates and surface of specimen during tests, was selected properly. As it was already mentioned, in order to validate the fixture work first part of hysteresis loop (the case of tension) was compared to the standard tensile curve (dotted line) obtained without usage of the fixture. As it is seen in Fig. 7, almost no differences exist between these curves, what means that the fixture enables proper operation, and therefore, reasonable results can be achieved.

The results of similar type of test carried out on the M63 brass under cyclic loading are presented in Fig. 10. The first cycle is illustrated by solid black line denoted as 1. The tensile stress–strain curve obtained under simple tension without the anti-buckling fixture usage (denoted as 2 in Fig. 6) is also shown in Fig. 10 (gray dotted line denoted as 2).

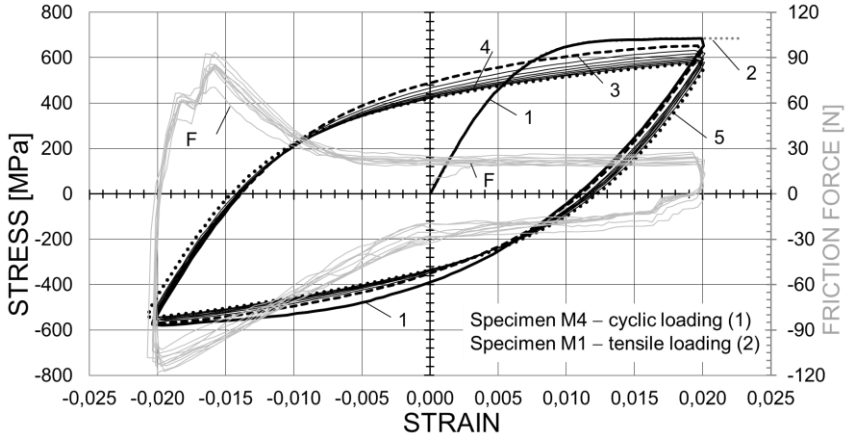

Figure 10: Hysteresis loops of the brass and friction force variation during test

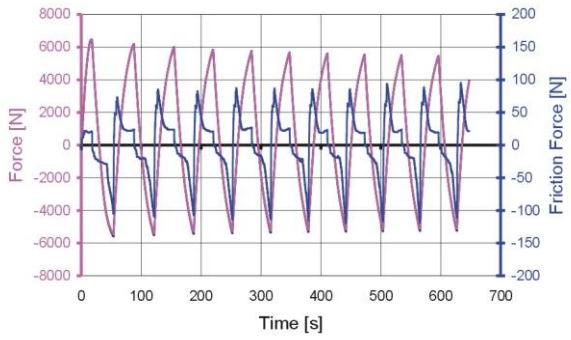

Figure 11: Variation of the specimen load and friction force versus time during cyclic loading (type 1) of the brass

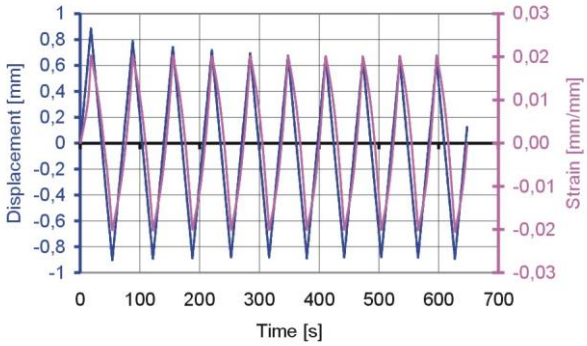

Figure 12: Variation of displacement and strain versus time during cyclic loading (type 1) of the brass

A second cycle is represented by black dashed line (3). Similarly as for the steel, the last two cycles - are denoted by black dotted lines (4 and 5). Figure 10 also presents an evolution of the friction force

(gray lines, denoted as F). The friction force is also shown as a function of time in Fig.11 as well as total force for all recorded cycles. Changes of strain, corresponding to the force variations, are shown in Fig. 12 for all cycles carried out. The strain amplitude for all cycles was kept constant. Contrary to the steel, the brass exhibited softening effect reflected by a significant decrease of the stress amplitude, especially in the first four cycles, Fig. 11.

A level of the friction force was also monitored during the test on brass. Its variation is presented in Figs. 10 and 11. The friction force has a similar course in all cycles and does not change clearly under tension and grow up at compression. It has to be emphasized, however, that the values of friction force were relatively small and they did not change the cyclic stress-strain characteristic.
Again, like for the steel, in order to check whether the fixture works correctly for large deformation under tension-compression cyclic loading the first tensile part of the stress-strain cyclic characteristic is compared to the tensile curve determined using the commercial extensometer. As it is clearly seen, Fig. 10, an excellent agreement is obtained. Both these characteristics coincide themselves, and therefore, it may be treated as confirmation of the good measurement capability of the fixture elaborated.

In the second scheme of test the cyclic loading were performed for strain level varying between 0 and -0.058 in the case of steel, or between -0.002 and -0.022 for brass. Also ten cycles were carried out, however, in this case the loading process started in compression direction. The results for steel are illustrated in Fig. 13. The first cycle is denoted as 1 and plotted by solid black line. Second and third cycles are represented by black thin lines denoted as 2 and 3, respectively. The last cycle are drawn by black dotted line denoted as 4.

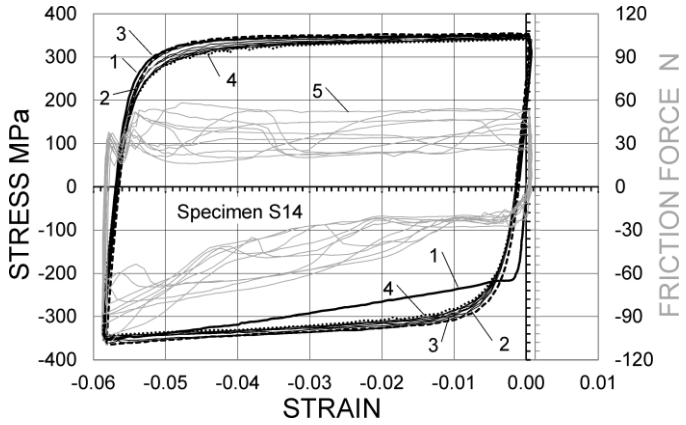

Figure 13: Hysteresis loops of the steel and friction force variation during test

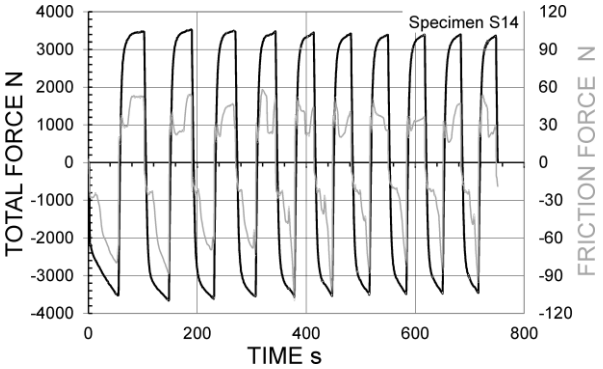

Figure 14: Variation of the specimen load and friction force versus time during cyclic loading (type 2) of the steel

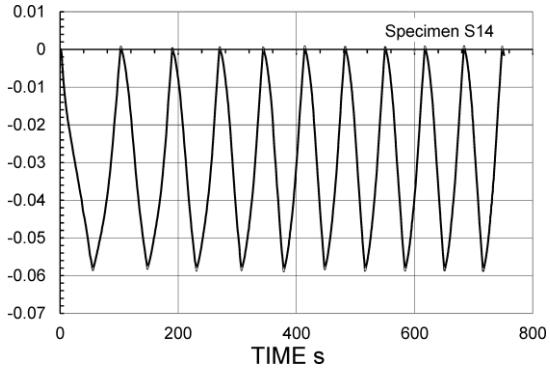

Figure 15: Variation of strain versus time during cyclic loading (type 2) of the steel

Courses of the friction force variation corresponding to the stress-strain loops are represented by gray lines denoted by 5. As in the first scheme, the friction force and total load are also shown as the functions of time in Fig.14 for all recorded cycles. The friction force has a similar course in all cycles

and grows up at compression due to transversal expansion of specimen and diminishes under reverse loading due to transversal shrink of the specimen. The test was also in displacement control and the corresponding changes of a strain measured by the extensometer attached in a middle part of the specimen are shown in Fig. 15 for all ten cycles. The strain amplitude for all cycles was kept constant. Similarly as for the first type test on the steel, the hardening effect can be observed when the courses of the first and second cycle are compared, Figs. 13 and 14. The results also exhibited the work hardening stagnation in a certain period of the reverse deformation. Similarly as for the symmetrical cycles, a level of the friction force was monitored during the test, Fig. 14, and again these data were subsequently used to correct the stress-strain diagram.

The results of second type of test carried out on the M63 brass under cyclic loading are presented in Figs. 16-18. Notation of cycles in Fig. 16 is exactly the same as that in Fig.13 applied.

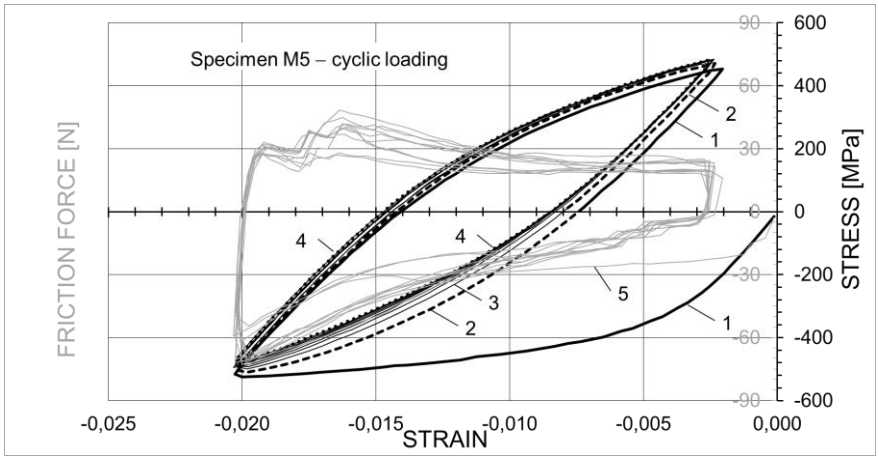

Figure 16: Hysteresis loops of the brass and friction force variation during test

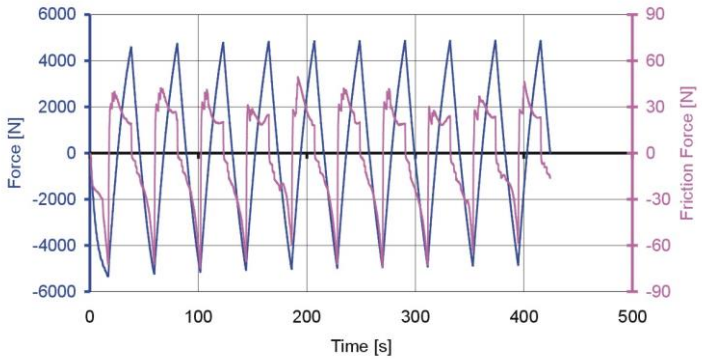

Figure 17: Variation of the specimen load and friction force versus time during cyclic loading (type 2) of the brass

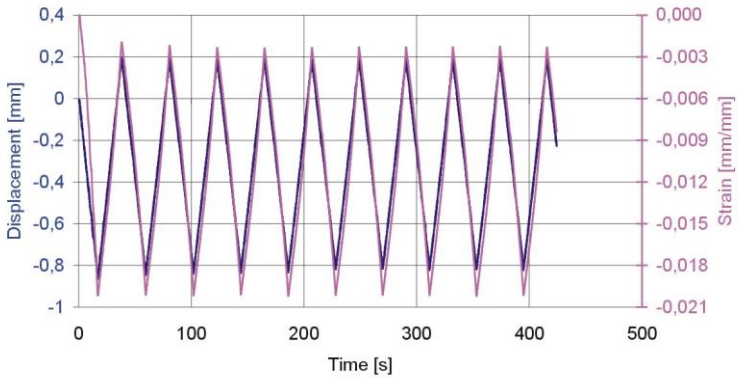

Figure 18: Variation of displacement and strain versus time during cyclic loading (type 2) of the brass

In comparison to the steel completely opposite behaviour can be observed. Instead of hardening the softening effect took place. It is most remarkable for the first two cycles. During subsequent cycles the saturation state was almost achieved, i.e. hysteresis loops coincide themselves. As it is clearly seen in Figs. 16 and 17, the friction force had rather low magnitudes. Moreover, its magnitude variations were much more repeatable in all cycles carried out than those obtained during steel testing in the similar loading conditions. As in the previous cases, the friction force variation data were subsequently used to correct the stress-strain characteristic of the brass tested.

4. Concluding remarks

Application of the proposed testing technique allowed tension-compression tests to be performed at the displacement amplitude within the range $\pm$5mm what corresponds to the maximum strain amplitude of $\pm$0.4 for the specimen gage length to be equal 12.5 mm. Taking into account all data captured by means of the new fixture one can conclude that the technique is promising with respect to providing data for modeling of cyclic deformation behavior for shell structures. It enables to avoid buckling during compression of specimens made of thin metal sheet. The fixture changes its length with specimen elongation or shrinkage during a test which allows application of cyclic load. The friction force, which is generated due to a movement of both parts of the fixture, is measured by the special strain gauge system during each test. It allows eliminating friction force influence on the stress-strain characteristics.

References

1. Standard methods of compression testing of metallic materials, ASTM E9-61.
2. C.S. Aitchison, L.B. Tuckerman, 1939, “The “pack” method for compressive tests of thin specimens of materials used in thin-wall structures”, *NACA*, 649.
3. J.A. Miller, 1946, “A fixture for compressive tests of thin sheet metal between lubricated steel guides”, *NACA* 1022.
4. K.R. Jackman, 1944, “Improved methods for determining the compression properties of sheet metal”, *Auto. Aviat. Indu.*, 90, 11, p. 36.
5. H. LaTour, S. Wolford, 1945, “Single-strip compression test for sheet materials”, *Proc. ASTM*, 45, p. 675.
6. P.E. Sandorff, R.K. Dillon, 1946, “Compressive stress-strain properties of some aircraft materials”, *Proc. ASTM*, 46, p.1039.
7. L. Dietrich, K. Turski, 1978, A new method of thin sheets testing under compression (in Polish), *Engineering Transactions*, 26, 1, 91-99.
8. W. Szczepiński Ed., 1990, Experimental Methods in Mechanics of Solids, PWN, Warszawa, Elsevier-Amsterdam-Oxford-New York-Tokyo.
9. Kuwabara T. (2007) Advances in experiments on metal sheets and tubes in support of constitutive modeling and forming simulations, Int. J. Plasticity **23**, pp. 385-419.
10. T. Kuwabara, Y. Kumanto, J. Ziegelheim, I. Kurasaki, 2009, “Tension-Compression asymmetry of phosphor bronze for electric parts and its effect on bending behavior”, *Int. J. Plasticity***,** 25, pp. 1759-1776.
11. J. Cao, W. Lee, H.S. Cheng, M. Seniw, H.P. Wang, K. Czung, 2009, “Experimental and numerical investigation of combined isotropic-kinematic hardening behavior of sheet metals”, *Int. J. Plasticity*, 25, pp. 942-972.
12. L. Dietrich, G. Socha, Z.L. Kowalewski, 2014, “Anti-buckling fixture for large deformation tension-compression cyclic loading of thin metal sheets”, *Strain Int. J. Exp. Mech.*, 50, pp. 174-183.
13. F. Yoshida, T. Uemori, K. Fujiwara, 2002, “Elastic-plastic behavior of steel sheets under in-plane cyclic tension-compression at large strain”, *Int. J. Plasticity* **18**, 5-6, pp. 633-659.